GEOPHYSICAL RESEARCH LETTERS, VOL. 28, NO. 5, PAGES 887-890, MARCH 1, 2001

Hot diamagnetic cavities upstream of the Martian bow shock

Marit Øieroset, David L. Mitchell, Tai D. Phan, and Robert P. Lin

Space Sciences Laboratory, University of California, Berkeley

Mario H. Acuña

Goddard Space Flight Center, Greenbelt, Maryland

Abstract. We present Mars Global Surveyor (MGS) observations of hot diamagnetic cavities upstream of the Martian bow shock. The events are characterized by a region of turbulent magnetic field, high electron temperature, and densities at or below the ambient solar wind density. The region of high temperature is flanked by layers of high magnetic field and electron density and is accompanied by a rotation in the interplanetary magnetic field (IMF). We suggest that the events are generated by interplanetary discontinuities interacting with the Martian bow shock, i.e., the events are the Martian counterpart to the hot flow anomalies observed upstream of the Earth's bow shock.

Introduction

A wide range of plasma and magnetic field perturbations are known to occur upstream of the Martian bow shock [e.g., *Riedler et al.*, 1989; *Russell et al.*, 1990; *Skalsky et al.*, 1992; *Barabash and Lundin*, 1993]. Waves at the proton gyro frequency have been associated with the pick-up of protons from the extended Martian exosphere [*Russell et al.*, 1990; *Barabash et al.*, 1991]. Strong turbulence near the crossings of the orbit of the Martian moon Phobos has been interpreted as a signature of the solar wind interaction with a gas/dust torus along the Phobos orbit [*Dubinin et al.*, 1990]. Foreshock turbulence and reflected ions and electrons have been observed when the interplanetary magnetic field (IMF) was connected to the bow shock [*Kiraly et al.*, 1991; *Barabash and Lundin*, 1993].

Although pick-up processes are present in the Martian foreshock, it has been suggested that the basic processes operating in the foreshocks of Earth and Mars are similar [*Skalsky et al.*, 1998 and references therein]. Hot flow anomalies (HFAs), earlier known as hot diamagnetic cavities [*Thomsen et al.*, 1986] or active current sheets [*Schwartz et al.*, 1985] have been observed in the Earth's foreshock region. HFAs are regions of hot tenuous plasma and turbulent magnetic field deflected from the surrounding solar wind flow and bounded by rotations in the magnetic field direction and regions of compressed, heated, and weakly shocked antisunward flowing plasma [*Fuselier et al.*, 1987].

Paper number 2000GL012289.
0094-8276/01/2000GL012289$05.00

Observations of HFAs near the Earth's bow shock are relatively rare [*Thomsen et al.*, 1988]. However, it has recently been pointed out that the events may be quite common but are only detected when a spacecraft is located in the immediate vicinity of the bow shock at the time of arrival of an interplanetary discontinuity [*Sibeck et al.*, 1999; *Schwartz et al.*, 2000].

In the present study we report observations of hot diamagnetic cavities in the solar wind near the Martian bow shock, using electron and magnetic field observations from the MGS spacecraft. We suggest that the cavities are hot flow anomalies generated by the same mechanisms as the corresponding events observed near the Earth's bow shock.

Observations

The magnetometer/electron reflectometer (MAG/ER) experiment onboard the MGS spacecraft is described in *Acuña et al.* [1998]. In the present study a magnetic field resolution of 0.3 seconds has been used. Calibration uncertainties

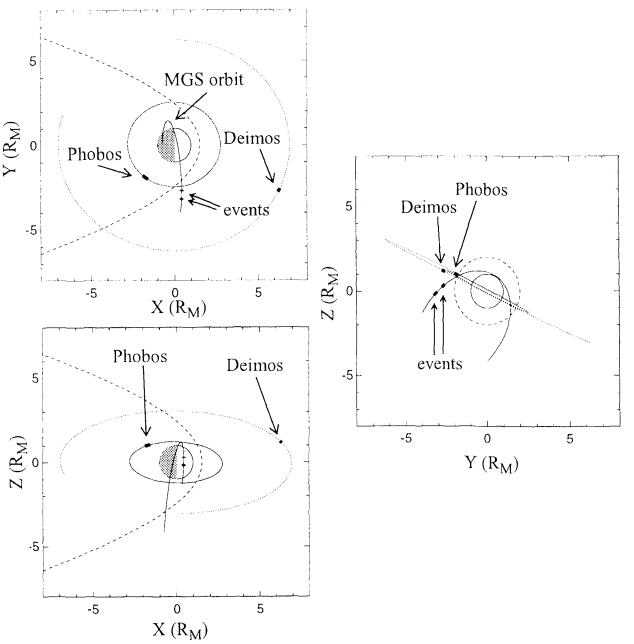

Figure 1. MGS SPO 443 in x-y, y-z, and x-z SSE coordinates (solid line). The two intervals of disturbances shown in Figure 2 are marked along the MGS orbit track. The orbits of Phobos and Deimos are plotted with the dotted lines, and the position of the moons at the time of the disturbances are marked.

of the order of 1 nT (when the spacecraft is in sunlight) preclude us from finding the absolute magnetic field direction in the solar wind, although relative changes in the direction over short ($\sim$ minutes) time intervals can be reliably estimated. The electron distribution function is measured in the range from $\sim$10 eV to 20 keV every 2 to 12 seconds, depending on the energy channel. The ER does not provide full 3D measurements and the electron density and temperature have been estimated by fitting the measurements to a Maxwellian distribution, assuming isotropy. The electron distributions are close to a Maxwellian in the solar wind, while there is a flux increase in the 30-800 eV range inside the (hot) magnetic cavities. The electron bulk flow velocity cannot be reliably estimated from the ER measurements.

We have used the sun synchronous ecliptic (SSE) coordinate system where X points from the center of the planet toward the Sun, the Z-direction is normal to the ecliptic plane, pointing north, and Y is directed opposite to the planet's orbital velocity.

The data are from science phasing orbit (SPO) 443 on July 22, 1998, when MGS was in an elliptical polar orbit with periapsis in the Martian ionosphere near the north pole. The MGS SPO 443 orbit is shown in Figure 1.

An overview of the MGS MAG/ER data from SPO 443 (13:13 - 14:42 UT) is shown in Figure 2. MGS crossed the bow shock from the magnetosheath into the solar wind at 14:06 UT. Ten minutes later (at 14:16 UT) the MAG/ER instrument recorded a $\sim$ 2 minute disturbance in both the energy flux (panel a) and the magnetic field magnitude and direction (panels d, e, and f). Fourteen minutes after the first disturbance ended a second interval (at 14:32 UT) with similar characteristics was recorded. The two disturbed intervals are marked along the orbit track in Figure 1.

Figure 3 shows the first disturbed interval in detail. The disturbance is characterized by a turbulent magnetic field and high electron temperature, while the density (panel b) remains at the same level as in the undisturbed solar wind. The interval of turbulent field is flanked by large magnetic field and electron density enhancements. The inner and outer boundaries of this edge region are marked by the red and the black dashed lines, respectively. A rotation in the IMF θ angle of 40° is associated with this event (panel f). We note that the magnetic field magnitude and the density enhancements on the edges of the event coincide, while the temperature increase occurs later but remains high in the core of the event.

Figure 4 shows the second interval of disturbance. This disturbance is composed of three separate events similar to the type shown in Figure 3. Each event is characterized by a hot turbulent field region flanked by magnetic field and density enhancements. The three events are marked with numbers 2, 3, and 4 in Figure 4. All events are associated with rotations ($\sim$ 40°, $\sim$ 20°, and $\sim$ 50° for event 2, 3, and 4, respectively) in the IMF θ angle. The amplitude of density, temperature, and magnetic field variations varies from one case to the next, but do not appear to be correlated with the size of the IMF rotation.

Discussion

As can be seen in Figure 2, the events are observed in close proximity to the bow shock. This raises the question whether the events are simply multiple bow shock crossings. A bow shock crossing is characterized by a simultaneous increase in magnetic field magnitude, plasma temperature, and plasma density. The events presented here (Figure 3 and 4) are flanked by a factor of 2.5 - 4 increases in the magnetic field magnitude, which is typical for bow shock crossings. However, the events differ from a bow shock crossing in that the density and temperature do not increase simultaneously. The high electron temperature region has the same density as in the undisturbed solar wind and the region is flanked by two high density and magnetic field layers. Hence the events are not simply multiple crossings of the Martian bow shock.

Foreshock turbulence is known to occur when the magnetic field is connected to the Martian bow shock [*Grard et al.*, 1991; *Skalsky et al*, 1992]. However, the factor of 2.5 - 4 increase in the magnetic field magnitude for the events presented here is larger than what has been observed for usual foreshock turbulence near Mars [*Russell et al.*, 1990; *Kiraly et al.*, 1991].

Outgassing from the Phobos and Deimos moons could conceivably give rise to measurable plasma and magnetic field variations [Ip and Banaszkiwicz, 1990]. However, the events shown in Figures 3 and 4 occurred far away ($>$ 3000 km) from the Phobos orbit and an explanation in terms of solar wind interaction with a Phobos gas/dust torus is unlikely.

The MGS spacecraft was located downstream of Deimos (see Figure 1) at the time of the events. For the first event MGS was located 9° off the Deimos-Sun line, and for the last three events MGS was 13° off. Based on Phobos-2 observations *Sauer et al.* [1995] estimated the Deimos Mach cone to have a 13° opening angle and attributed isolated magnetic field perturbations to crossings of the Deimos Mach cone. If the events presented here were caused by the solar wind-Deimos interaction it would imply a Deimos Mach cone opening angle of up to 26°. We find such a large Mach cone unlikely. Besides, the signatures reported as Phobos and Deimos events [*Dubinin et al.*, 1990; *Sauer et al.*, 1995] are substantially different from the present events. They do not show hot plasma flanked by large magnetic field and density enhancements.

Another possibility is that Deimos and the spacecraft are magnetically connected. Deimos and the magnetic field vector measured at the spacecraft appear to lie in different planes (separated in Z). However, we can not conclusively rule out a magnetic connection between the spacecraft and Deimos as a cause of the event because of the uncertainty in the measurements of the solar wind magnetic field direction (see above).

We believe that hot flow anomalies (HFAs) are a more likely explanation for the present events. The hot plasma structures observed upstream of Mars (Figures 3 and 4) are characterized by a central region of turbulent magnetic field and an associated increase in electron temperature, similar

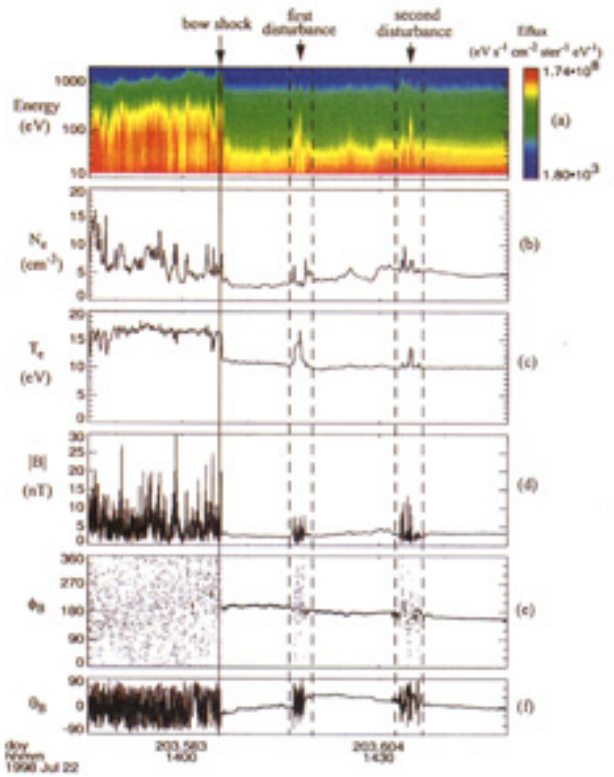

Figure 2. MGS MAG/ER data from orbit (SPO) 443. The electron energy spectrogram (energy flux) is shown in panel (a), while panel (b) and (c) show the electron density (N_e) and temperature (T_e), respectively, both obtained by Maxwellian fitting. The magnetic field observations are given in panels (d) - (f) as the magnetic field magnitude ($|B|$), the ϕ angle, and the θ angle, where $\phi_B = \arctan \frac{B_y}{B_x}$ and $\theta_B = \arcsin \frac{B_z}{|B|}$.

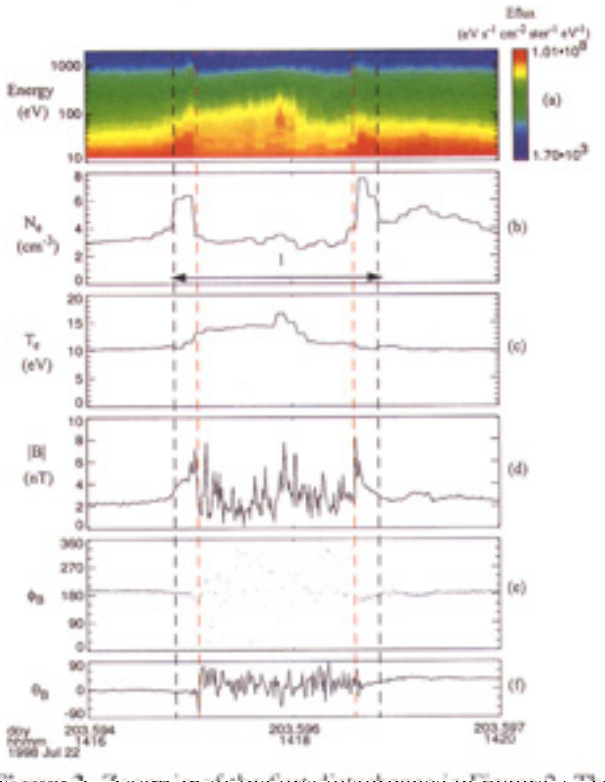

Figure 3. Zoom-in of the first disturbance in Figure 2. The hot central region is marked by the red dashed lines while the black dashed lines mark the outer boundaries of the edge regions.

to the HFAs observed upstream of the Earth [*Schwartz et al.*, 1985; *Thomsen et al.*, 1986]. The central region of the events is flanked by strong magnetic field and high density, as was also the case for the terrestrial HFAs [*Schwarz et al.*, 1985; *Thomsen et al.*, 1986].

All four events presented here are associated with rotations in the IMF. Earlier observations have revealed that HFAs are associated with directional discontinuities in the IMF [*Paschmann et al.*, 1988; *Schwartz et al.*, 1988]. The presence of flow deflection, typical of terrestrial HFAs cannot be verified for the MGS events because of the 2D nature of the electron measurements.

Based on the close similarity in the plasma and field properties of the present events and the Earth's events, we thus suggest that these events are the Martian counterpart of the terrestrial HFAs. The close association of the occurrence of HFAs and IMF rotational discontinuities indicates that the HFAs are generated by an interaction between an interplanetary current sheet and the bow shock [*Schwarz et al.*, 1985; *Thomas et al.*, 1991; *Lin et al.*, 1997]. A hot diamagnetic cavity, or HFA, form when ions initially reflected at the bow shock interact with the current sheet embedded in the shock to produce a high-temperature region [*Thomas et al.*, 1991;

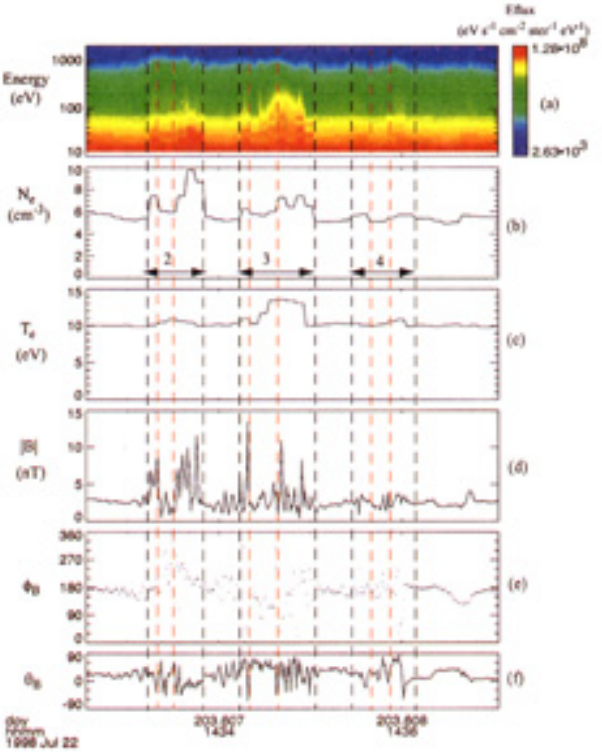

Figure 4. Zoom-in of the second disturbance in Figure 2. The hot central regions are marked by the red dashed lines while the black dashed lines mark the outer boundaries of the edge regions.

Lin, 1997]. The region of high temperature then expands against the surrounding medium, excluding the incoming solar wind with weak shock waves, causing a decrease in the density and magnetic field in the regions of high temperature [*Thomas et al.*, 1991].

Observations of hot diamagnetic cavities upstream of the Martian bow shock are rare. Out of ~250 bow shock crossings only five candidate events were found in addition to the four events presented here. This should not be surprising since it has been shown also for the Earth's case that the observations of HFAs are also rare [*Thomsen et al.*, 1988]. The detection of an HFA may require that the spacecraft be located near the intersection point of the interplanetary current sheet and the bow shock at the time of intersection [*Sibeck et al.*, 1999].

Conclusions

We have presented observations of hot diamagnetic cavities upstream of the Martian bow shock. We suggest that they are most likely the Martian counterpart to the hot flow anomalies (or hot diamagnetic cavities) observed upstream of the Earth's bow shock and generated by IMF discontinuities interacting with the bow shock. The existence of these events upstream of both the Martian and terrestrial bow shock suggests that the two bow shocks have similar properties although the nature of the two solar wind obstacles (one with and one without a magnetosphere) are quite different. The existence of HFAs upstream of both the terrestrial and the Martian bow shock also eliminates the possibility that HFAs are generated at the planetary magnetopause, since Mars does not have a magnetosphere.

Finally, the HFAs upstream of the Earth have been observed closer to the subsolar region [e.g., *Schwartz et al.*, 1988], while the Martian events presented here are observed at the dawn flank of the bow shock, near the terminator plane. Hence, the present observations imply that hot flow anomalies are present not only upstream of the subsolar bow shock, but also at the flank where the shock is weaker.

Acknowledgments. We thank Konrad Sauer for helpful discussions and Stephen Fuselier for comments on the manuscript. This research was funded by NASA grant NAG 5-959 at U. C. Berkeley.

References

Acuña, M. H. et al., Magnetic field and plasma observations at Mars: Initial results from the Mars Global Surveyor mission, *Science, 279*, 1676, 1998.

Barabash, S., and R. Lundin, Reflected ions near Mars: Phobos-2 observations, *Geophys. Res. Lett., 20*, 787, 1993.

Barabash, S. et al., Picked-up protons near Mars: Phobos observations, *Geophys. Res. Lett., 18*, 1805, 1991.

Dubinin, E. et al., Indirect evidence for a gas/dust torus along the Phobos orbit, *Geophys. Res. Lett., 17*, 861, 1990.

Fuselier, S. A. et al., Fast shocks at the edges of hot diamagnetic cavities upstream from the Earth's bow shock, *J. Geophys. Research, 92*, 3187, 1987.

Grard, R. et al., Plasma and waves around Mars, *Planet. Space Sci., 39*, 89, 1991.

Ip, W.-H., and M. Banaszkiwicz, On the dust/gas tori of Phobos and Deimos, *Geophys. Res. Lett., 17*, 857, 1990.

Kiraly, P. et al., The HARP plasma experiment on-board the Phobos 2 spacecraft - Preliminary results, *Planet. Space Sci., 39*, 139, 1991.

Lin, Y., Generation of anomalous flows near the bow shock by its interaction with interplanetary discontinuities, *J. Geophys. Research, 102*, 24,265, 1997.

Paschmann, G. et al., Three-dimensional plasma structures with anomalous flow directions near the Earth's bow shock, *J. Geophys. Research, 93*, 11,279, 1988.

Riedler, W. et al., Magnetic fields near Mars: First results, *Nature, 341*, 604, 1989.

Russell, C. T. et al., Upstream waves at Mars, *Geophys. Res. Lett., 17*, 897, 1990

Sauer, K. et al., Deimos: An obstacle to the solar wind, *Science, 269*, 1075, 1995.

Schwarz, S. J. et al. An active current sheet in the solar wind, *Nature, 318*, 269, 1985.

Schwartz, S. J. et al., Active current sheets near the Earth's bow shock, *J. Geophys. Research, 93*, 11,295, 1988.

Schwartz, S. J. et al., Conditions for the formation of hot flow anomalies at Earth's bow shock, *J. Geophys. Research, 105*, 12,639, 2000.

Sibeck, D. G. et al., Comprehensive study of the magnetospheric response to a hot flow anomaly, *J. Geophys. Research, 104*, 4577, 1999.

Skalsky, A. et al., The Martian bow shock: Wave observations in the upstream region, *J. Geophys. Research, 97*, 2927, 1992.

Skalsky, A. et al., Wave observations at the foreshock boundary in the near-Mars space, *Earth Planet. and Space, 50*, 439, 1998.

Thomas, V. A. et al., Hybrid simulation of the formation of a hot flow anomaly, *J. Geophys. Research, 96*, 11,625, 1991.

Thomsen, M. F. et al., Hot, diamagnetic cavities upstream from the Earth's bow shock, *J. Geophys. Research, 91*, 2961, 1986.

Thomsen, M. F. et al., On the origin of hot diamagnetic cavities near the Earth's bow shock, *J. Geophys. Research, 93*, 11,311, 1988.

R. P. Lin, D. L. Mitchell, M. Øieroset, T. D. Phan, Space Sciences Laboratory, University of California, Berkeley, CA 94720. (oieroset@ssl.berkeley.edu)

M. H. Acuña, NASA Goddard Space Flight Center, Code 695, Greenbelt, MD 20771

(Received September 1, 2000; revised November 1, 2000; accepted December 6, 2000.)